

Phosphine promoted substituent redistribution reactions of B-chlorocatechol borane: molecular structures of ClBcat, BrBcat and L·ClBcat (cat = 1,2-O₂C₆H₄; L = PMe₃, PEt₃, PBu^t₃, PCy₃, NEt₃)[†]

R. Benjamin Coapes,^a Fabio E. S. Souza,^b Mark A. Fox,^a Andrei S. Batsanov,^a Andrés E. Goeta,^a Dimitrii S. Yufit,^a Michael A. Leech,^a Judith A. K. Howard,^a Andrew J. Scott,^c William Clegg^c and Todd B. Marder^{*ab}

^a Department of Chemistry, University of Durham, Durham, UK DH1 3LE.
E-mail: todd.marder@durham.ac.uk

^b Department of Chemistry, University of Waterloo, Waterloo, Ontario, N2L 3G1, Canada

^c Department of Chemistry, University of Newcastle upon Tyne, Newcastle upon Tyne, UK NE1 7RU

Received 15th December 2000, Accepted 19th February 2001

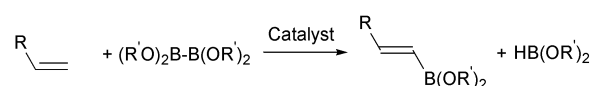
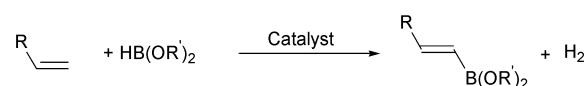
First published as an Advance Article on the web 28th March 2001

In order to evaluate the potential for side reactions when using B-chlorocatechol borane (ClBcat) in stoichiometric or catalytic transformations involving metal phosphine complexes, we examined the interaction between ClBcat and a series of PR₃ compounds. Reactions of ClBcat with the basic phosphines PMe₃, PEt₃, PMe₂Ph and PBu^t₃, in exactly 1 : 1 stoichiometry, all afforded crystalline adducts of the form R₃P·ClBcat, which have been characterised spectroscopically. All display broad singlets at room temperature in both ¹¹B{¹H} and ³¹P{¹H} NMR spectra with no B–P coupling observed. The low temperature ¹¹B{¹H} and ³¹P{¹H} NMR spectra, however, do show B–P coupling, suggesting rapid dissociation at room temperature. The compounds ClBcat, BrBcat, and the adducts between ClBcat and PMe₃, PEt₃ and PBu^t₃ have been characterised by single crystal X-ray diffraction. In ClBcat and BrBcat, the halogen contributes little π-bonding to boron as the B–O bond lengths are identical in both compounds. The reaction of ClBcat with a small excess of PCy₃ yielded Cy₃P·ClBcat, which has also been characterised by single crystal X-ray diffraction and shows considerable distortion. The reaction between ClBcat and the less basic phosphines PPh₃ and PPh₂Me yielded only the redistribution products R₃P·BCl₃ and B₂cat₃. In fact, reaction of all of the phosphines with an excess of ClBcat gave only redistribution products, although there was evidence for an intermediate in the ¹¹B{¹H} NMR spectra, with PMe₃ and PEt₃. The isolated R₃P·ClBcat adducts proved unstable, even at low temperature in the solid state, eventually leading to R₃P·BCl₃ and B₂cat₃. Reaction of ClBcat with NEt₃ afforded Et₃N·ClBcat, which was characterised spectroscopically and by single crystal X-ray diffraction. This adduct is stable both in solution and in the solid state.

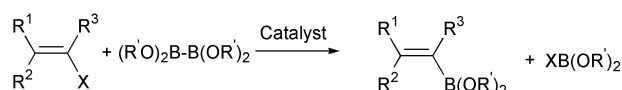
Introduction

There are now many examples of the transition metal catalysed addition of boron compounds to various unsaturated substrates, in reactions such as hydroboration,^{1–3} diboration,^{4,5} dehydrogenative borylation of alkenes,^{6–16} silylboration,^{17,18} thioboration,^{19–21} stannylboration,^{22,23} reactions of aryl or vinyl halides or triflates with B₂(OR)₄ or HB(OR)₂,^{24–34} and direct activation of C–H bonds in alkanes and arenes.^{35–41} These reactions all involve an Ecat or EBP_{in} species (E = H, Bcat, Bpin, SR, SiR₃, SnR₃, cat = 1,2-O₂C₆H₄, pin = OCMe₂CMe₂O), and several reviews highlight studies of the intermediate metal–boryl species.^{42–45} Whilst dehydrogenative borylation of alkenes to vinylboronate esters using HB(OR)₂ or B₂(OR)₄ is known,^{6–16} a more attractive and less expensive variant would be the use of a commercially available ClB(OR)₂ reagent, such as ClBcat, and base in a boron analogue of the Heck reaction (Scheme 1). Such a reaction would likely entail the oxidative addition of ClBcat to a metal centre,⁴⁶ the use of tertiary amines as base, and the use of phosphine ligands on a late transition metal catalyst. Hence, there is a need to ascertain what, if any, reactivity there is between ClBcat and R₃P or R₃N, as it is known that nucleophiles,^{47–49} including phosphines,⁴⁹ can

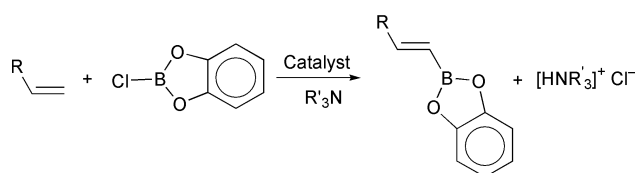
Dehydrogenative Borylation



Cross-Coupling



Proposed Boron Analogue of Heck Reaction



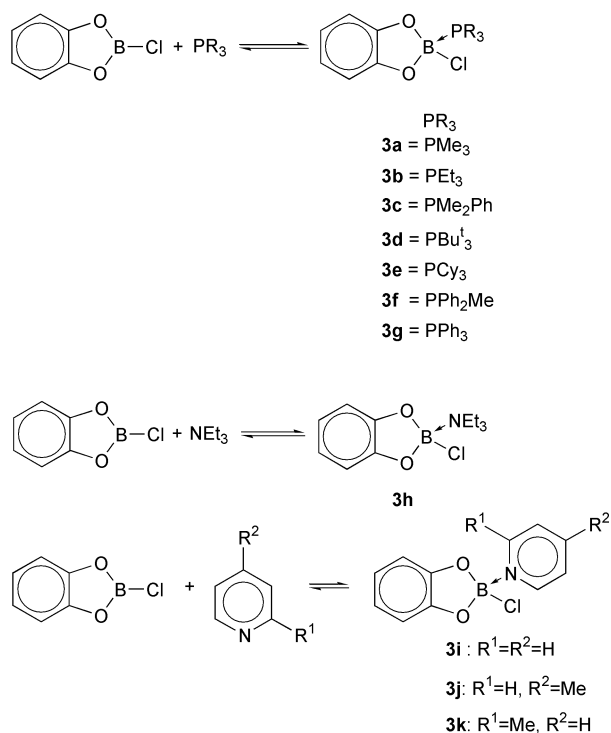
Scheme 1 Catalysed routes to vinylboronate esters from alkenes.

[†] B-chlorocatechol borane = 2-chloro-1,3,2-benzodioxaborole.

Table 2 Ambient and low temperature (−40 °C) ^{31}P and ^{11}B NMR data for **1** and **3a–e**

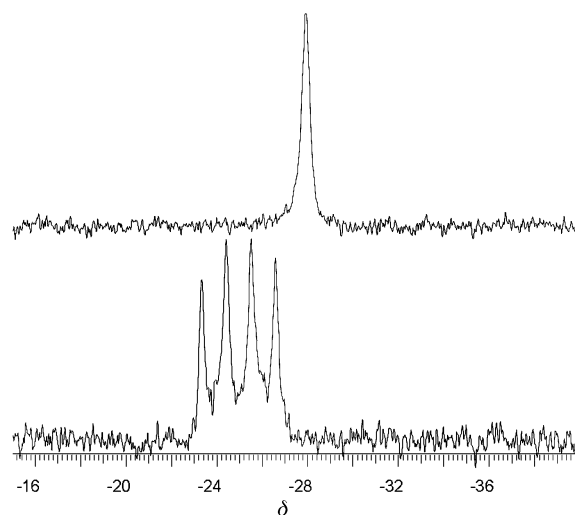
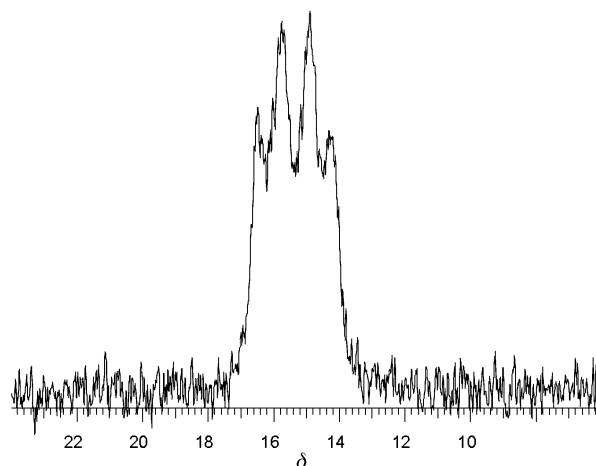
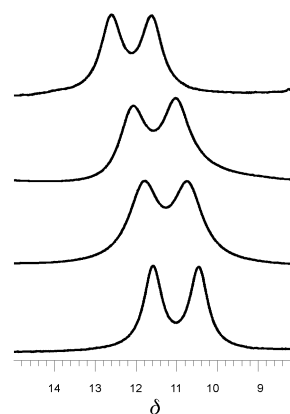
Compound	^{31}P shift (ppm) at ambient temperature	^{31}P shift (ppm) at −40 °C	^{31}P shift (ppm) of free phosphine	^{11}B shift (ppm) at ambient temperature	^{11}B shift (ppm) at −40 °C
1				28.4	
3a	−27.9	−24.9	−61.4	11.1	11.0
3b	1.4	6.8	−19.9	11.4	11.3
3c	−29.8	−22.8	−45.4	11.8	11.6
3d	25.5	15.3	61.8	15.8	12.1
3e	−3.3	−6.6	10.9	12.2	11.8

that of free phosphine (higher frequency for **3a**, **3b** and **3c**, lower for **3d**), with no evidence of any coupling to boron (Table 2). The absence of observed coupling, and the width of the peak, compared to the sharp signals displayed by the free phosphines, both point to the adduct being in equilibrium with free ClBcat and phosphine at this temperature (Scheme 2).

**Scheme 2** Adduct formation from reaction of ClBcat and LR_3 .

The low temperature $^{31}\text{P}\{^1\text{H}\}$ NMR spectra of **3a**, **3b** and **3c**, all show a further shift to higher frequency with evidence of P–B coupling, at −20 °C, and display an approximate 1 : 1 : 1 : 1 quartet at −40 °C, as expected for coupling to ^{11}B ($I = 3/2$), with $J_{\text{B-P}} = 175, 169$ and 166 Hz for **3a**, **3b** and **3c**, respectively (Fig. 3). Coupling to ^{10}B is not observed. Adduct **3d**, however, shows no P–B coupling at −20 °C, but shifts further to lower frequency and shows coupling at −40 °C and below, with $J_{\text{B-P}} = 160$ Hz, and with a splitting pattern which is, approximately, a 1 : 2 : 2 : 1 quartet (Fig. 4). This, it seems likely, is due to the partial thermal decoupling of the boron quadrupole which results in the quartet collapsing towards a singlet, with the two outside peaks decreasing in size, and the two central peaks growing in intensity. The spectrum taken at −60 °C shows a more exaggerated distortion from 1 : 1 : 1 : 1 and is consistent with the thermal decoupling of ^{11}B .

The ambient temperature $^{11}\text{B}\{^1\text{H}\}$ NMR spectra of **3a**, **3b**, **3c** and **3d** all display a peak considerably shifted to lower frequency (Table 2) from the position of free ClBcat (δ 28.4) with, as expected, no evidence of coupling to ^{31}P . The low temperature $^{11}\text{B}\{^1\text{H}\}$ NMR spectra at −40 °C, however, all show broad doublets at a frequency shifted slightly further away from free ClBcat (Fig. 5) and give B–P coupling constants of 178, 167, 166 and 158 Hz for **3a**, **3b**, **3c** and **3d** respectively.

**Fig. 3** $^{31}\text{P}\{^1\text{H}\}$ NMR spectra of **3a** in toluene–10% C_6D_6 at ambient temperature (top) and at −40 °C.**Fig. 4** $^{31}\text{P}\{^1\text{H}\}$ NMR spectrum of **3d** in toluene–10% C_6D_6 at −40 °C.**Fig. 5** $^{11}\text{B}\{^1\text{H}\}$ NMR spectra of **3a** (bottom), **3b**, **3c** and **3d** (top) in toluene–10% C_6D_6 at −40 °C.

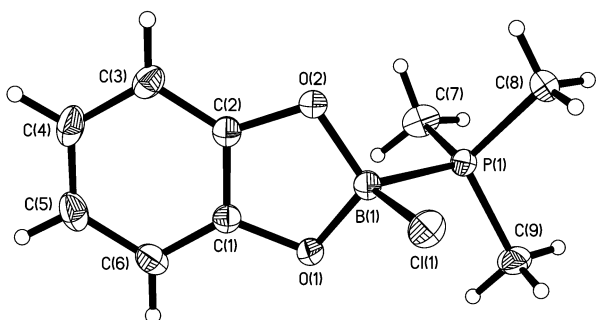


Fig. 6 Structure of one of the two crystallographically independent molecules of $\text{Me}_3\text{P}\cdot\text{ClBcat}$, **3a**.

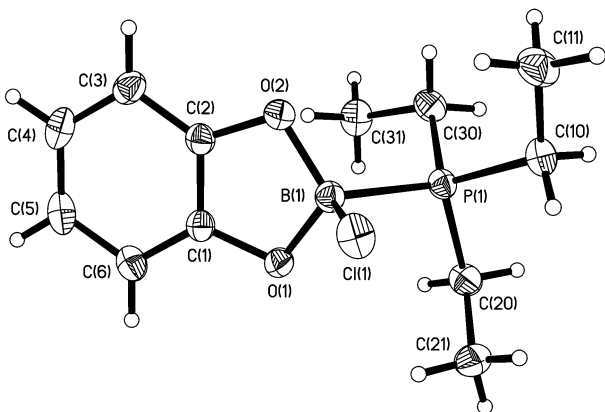


Fig. 7 Structure of $\text{Et}_3\text{P}\cdot\text{ClBcat}$ **3b**.

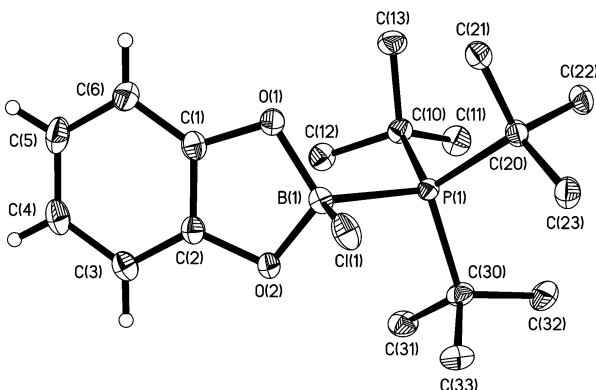


Fig. 8 Structure of $\text{Bu}_3\text{P}\cdot\text{ClBcat}$ **3d**. Hydrogens on the Bu^t groups are omitted for clarity.

It is clear from the temperature dependence of the ^{31}P and ^{11}B shifts in Table 2, that the adducts **3a–e** are mostly bound in solution at ambient temperature. However, **3d** shows substantial shifts in both ^{31}P and ^{11}B resonances as a function of temperature suggesting more dissociation than the others, consistent with PBu_3 having a particularly large cone angle (*vide infra*).

It was noticed that the $^3J_{\text{H-P}}$ coupling constant in **3b** was 16 Hz whereas that for **3d** was 11 Hz. A low temperature ^1H NMR spectrum of **3d** at -40°C , however, gave $^3J_{\text{H-P}} = 15$ Hz, with the peak shifted by *ca.* 0.1 ppm to δ 1.65, further indicating that the adducts are undergoing rapid exchange at room temperature. There is also a change in coupling constant from that in the free phosphine ($^3J_{\text{H-P}} = 10$ Hz), indicating that the increase in coupling constant gives a measure of the association between the phosphine and **1**.

The single crystal structures of **3a**, **3b** and **3d** have been determined by X-ray diffraction; molecular structures are shown in Figs. 6–8, with bond distances and angles provided in Table 1. The B–P bond lengths for **3a**, **3b** and **3d** are 1.967(2) (average for the two independent molecules), 2.008(2) and 2.048(2) Å, respectively.

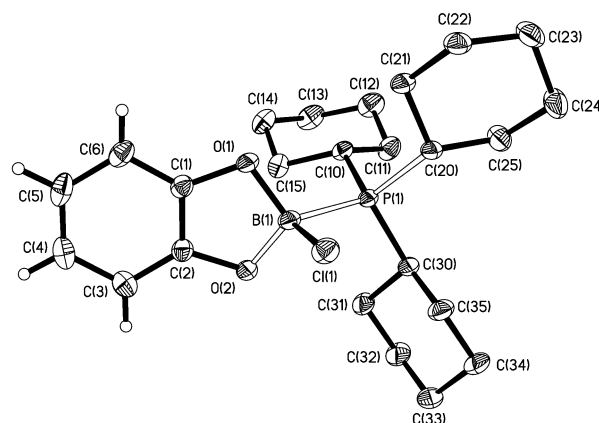


Fig. 9 Structure of $\text{Cy}_3\text{P}\cdot\text{ClBcat}$ **3e**. Hydrogens on the Cy rings omitted for clarity. Hollow bonds highlight distances which deviate significantly from those in other adducts.

The increase in B–P bond lengths correlates with the decrease in B–P coupling constants and the apparent stability of the adducts. These trends are probably due to a compromise between basicity,⁵¹ measured as the acidity of the conjugate acid $[\text{HPR}_3]^+$, and cone angle⁵² of the phosphine. For example, the $\text{p}K_{\text{a}}$ of $[\text{HPBu}_3]^+$ is 11.4 vs. 8.65 for $[\text{HPMe}_3]^+$. The cone angle of PBu_3 , however, is 182° vs. 118° for PMe_3 , and so $\text{Me}_3\text{P}\cdot\text{ClBcat}$ contains the stronger B–P interaction. Similarly, $[\text{HPEt}_3]^+$ has a $\text{p}K_{\text{a}}$ of 8.69, very close to that of $[\text{HPMe}_3]^+$, but a cone angle of 132° and so forms a weaker adduct than PMe_3 . Although purely empirical, this does provide a good guide to explaining the adduct stabilities, structural and spectroscopic parameters.

As expected, the increase in coordination number at boron from three to four with change in hybridisation from sp^2 to sp^3 , and the concomitant increase in steric repulsion, cause a lengthening of the B–Cl and B–O bonds from those in **1**. The B–Cl bonds lengthen by *ca.* 10% from 1.744(3) Å in **1** to 1.914(2), 1.925(2) and 1.914(2) Å in **3a**, **3b** and **3d**, respectively, and the B–O bonds lengthen by *ca.* 6% [an average of 1.461(2) Å]. Note also that O–B(p_z) π -bonding should be minimal in the four-coordinate adducts as B(p_z) is now tied up in σ -bonding to P. The boron atom is also ‘tipped’ out of the plane of the catechol ring, by between *ca.* 0.11 and 0.20 Å (Table 1). The B–P bond lengths in Table 1 are comparable with those in the analogous $\text{R}_3\text{P}\cdot\text{BCl}_3$ adducts; for example the B–P bond lengths in $\text{Me}_3\text{P}\cdot\text{BCl}_3$, $\text{Et}_3\text{P}\cdot\text{BCl}_3$, and $\text{Bu}_3\text{P}\cdot\text{BCl}_3$ are 1.957(5), 1.981(3) and 2.055(2) Å respectively.⁵⁰

The 1 : 1 reaction of **1** with PCy_3 yielded a mixture of products, as indicated by $^{11}\text{B}\{^1\text{H}\}$ NMR spectroscopy, including $\text{Cy}_3\text{P}\cdot\text{ClBcat}$ **3e** (δ 12.1), the redistribution products $\text{Cy}_3\text{P}\cdot\text{BCl}_3$ (δ 3.7, d, $J_{\text{B-P}} = 147$ Hz) and B_2cat_3 (δ 23.4) and additional peaks at δ 21.9 and 11.1. In contrast, the $^{31}\text{P}\{^1\text{H}\}$ NMR spectrum showed only a broad peak due to **3e** at δ –3.3 which presumably obscures the signal due to the $\text{Cy}_3\text{P}\cdot\text{BCl}_3$ adduct (δ 3.2, q, $J_{\text{P-B}} = 147$ Hz).⁵⁰ A 1.1 : 1 reaction of PCy_3 and **1** gave a small amount of a white precipitate of **3e**, recrystallisation of which yielded single crystals. The $^{11}\text{B}\{^1\text{H}\}$ NMR spectrum showed that the crystals were **3e**, but an additional peak was observed at δ 22.2. The level of this impurity changes, however, depending on concentration of the sample and on the time in solution, so the formation of the impurity would seem to take place in solution. The low temperature $^{31}\text{P}\{^1\text{H}\}$ NMR spectrum of **3e** showed some coupling at -20°C , and, at -40°C , displayed a broad 1 : 2 : 2 : 1 quartet, similar to **3d**, at δ –6.6, with $J_{\text{P-B}} = 159$ Hz. The low temperature $^{11}\text{B}\{^1\text{H}\}$ NMR spectrum at -40°C showed a doublet at δ 11.8 with $J_{\text{B-P}} = 160$ Hz.

The molecular structure of **3e** has been obtained (Fig. 9) and comparison of the structures of the four adducts **3a**, **3b**, **3d** and **3e**, determined by X-ray crystallography, reveals that of **3e** to be

Table 3 Comparison of selected bond lengths (Å) and energies between experimental and optimised (HF/6-31G*) geometries of R₃P·ClBcat adducts

R		B–O	B–Cl	B–P	P–C	E _n /hartrees	ΔE ^a /kJ mol ⁻¹
Me	Exptl.	1.46, 1.46	1.91	1.97	1.80, 1.80, 1.79	–1323.14176	10.0 (7.5)
	Theory	1.44, 1.44	1.89	2.03	1.82, 1.82, 1.82	–1323.14556	
Et	Exptl.	1.46, 1.46	1.93	2.01	1.82, 1.82, 1.82	–1440.23448	16.7 (11.3)
	Theory	1.44, 1.44	1.89	2.04	1.84, 1.83, 1.84	–1440.24085	
Bu ^t	Exptl.	1.46, 1.47	1.91	2.05	1.90, 1.90, 1.91	–1674.38484	11.7 (6.7)
	Theory	1.44, 1.44	1.91	2.08	1.92, 1.92, 1.93	–1674.38936	
Cy	Exptl.	1.47, 1.41	1.99	1.99	1.77, 1.87, 1.88	–1905.12893	87.4 (46.0)
	Theory	1.44, 1.44	1.91	2.05	1.86, 1.86, 1.87	–1905.16231	

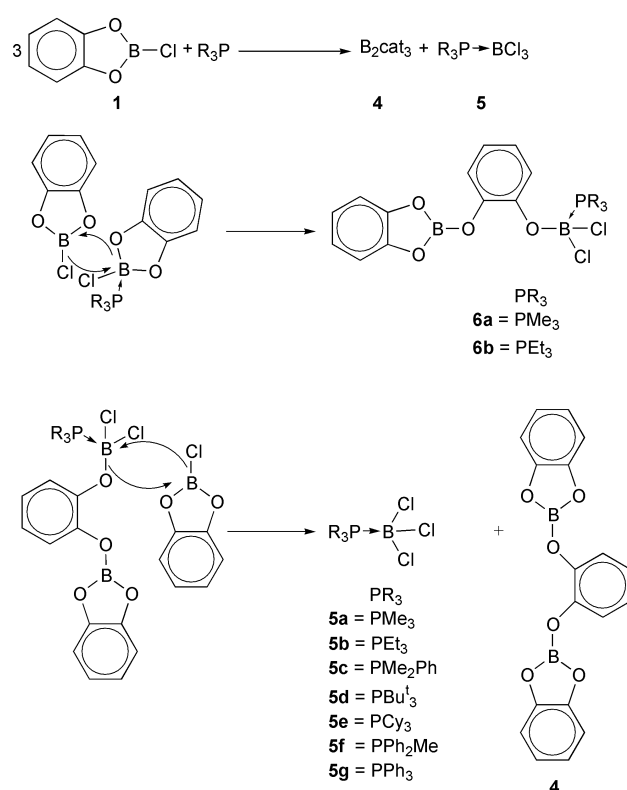
^a Values (× 10⁻³) in parentheses are generated by ΔE/E(theory) for a more realistic comparison.

quite different from the others. Compared to the analogous bond distances found in **3a**, **3b** and **3d**, the most obvious differences in the geometry of **3e** are the B–O(2) bond, shortened by 0.05 Å to 1.408(2) Å, the B–Cl bond, lengthened by 0.06 Å to 1.995(2) Å, and the P–B bond length of 1.991(2) Å being shorter than all but that in **3a**. Additionally, P–C(20), at 1.768(2) Å, is over 0.1 Å shorter than P–C(10), at 1.884(2) Å, and P–C(30), at 1.870(2) Å. There is also further distortion throughout the catechol group, most significantly C(2)–O(2) and C(1)–C(2) when compared to values obtained from the other adducts, and the boron is further ‘tipped’ out of the plane of the catechol group by 0.25 Å.

In an attempt to understand why **3e** has a distorted molecular structure in the solid state relative to the other adducts, geometry optimisations (at the HF/6-31G* level with Gaussian 94⁵³) from the X-ray structural data of all four adducts were carried out. Table 3 contains selected bond lengths of experimental and optimised ‘gas-phase’ geometries for these adducts, and these values show very good agreement in all cases except **3e**. Energy differences between experimental (with their hydrogens optimised as they are not located accurately by X-ray crystallography) and optimised geometries in these adducts reveal a relatively large value of 87 kJ mol⁻¹ for **3e** compared with much smaller values of ca. 10–17 kJ mol⁻¹ for **3a**, **3b** and **3d**. Even allowing for the fact that the total energy of **3e** is larger than those of the other adducts, the energy difference for **3e** is substantial. We find no obvious intramolecular reasons for the distortions observed for **3e** in the solid state.

Crystal packing forces must therefore account for a large part of the distortion and the associated energy difference computed theoretically between the optimised and observed geometries. Examination of the crystal structure of **3e** revealed close Cl···H intermolecular distances of 2.9 Å involving cyclohexyl hydrogens. A Cambridge Structural Database Search⁵⁴ for B–Cl···H–C interactions gave an average distance of 3.4 Å from 166 compounds, very few being shorter than 2.9 Å. Thus, intermolecular packing forces appear to be responsible for the observed differences in the molecular structure in the crystal of the PCy₃ adduct compared to its optimised ‘gas-phase’ geometry. The experimental solid state structures of the other adducts are largely unaffected by packing forces, as they correspond very well with their optimised ‘gas-phase’ geometries, obtained from the *ab initio* molecular orbital calculations.

The 1 : 1 reactions of **1** with the phosphines PPh₂Me and PPh₃ both yielded the redistribution products B₂cat₃ **4** and R₃P·BCl₃ **5f** and **5g**, as shown in Scheme 3. The reactions were not instantaneous, however, and the ¹¹B{¹H} NMR spectrum of each, when taken after 1 h, showed B₂cat₃, a doublet due to **5f** or **5g**, and another peak due to unreacted **1**. This peak was shifted by ca. 0.5 ppm to lower frequency from the expected position of free **1**, most likely indicating a very weak interaction between phosphine and **1**. When left for 24 h, the ¹¹B{¹H} NMR spectra showed only peaks due to B₂cat₃ **4** and **5f** or **5g**. In these two cases, it seems likely that R₃P·ClBcat adducts do form but that the interactions are very weak due predominantly



Scheme 3 Equation and proposed mechanism for boron substituent redistribution of R₃P·ClBcat in the presence of an excess of ClBcat.

to low phosphine basicity (PPh₂Me, pK_a = 4.57, PPh₃, pK_a = 2.73), and the large cone angle (PPh₂Me = 136°, PPh₃ = 145°).

Interestingly, even for those R₃P·ClBcat adducts that were isolated, boron substituent redistribution took place over a period of several weeks in the solid state at –30 °C. It is clear, therefore, that the thermodynamic products are **4** and R₃P·BCl₃, with the phosphine adducts of **1** being only kinetically stable. The mechanism shown in Scheme 3 is proposed for the redistribution reaction. In this mechanism, a molecule of **1** with coordinated phosphine reacts with an uncoordinated molecule of **1**, first forming an intermediate, **6**, which then reacts with a further uncoordinated molecule of **1** to form **4** and the R₃P·BCl₃ adduct **5**.

This mechanism is based on the fact that once a phosphine is bound to ClBcat, the oxygen atoms, having lost the ability to π-bond to boron, become nucleophilic. Attack at the electrophilic boron of an uncoordinated ClBcat leads to ring opening of the original BO₂ moiety and subsequent transfer of a Cl⁻ between the two boron centres. Note that the electrophilic attack of ClBcat on an oxygen of the R₃P·ClBcat adduct with ring opening is analogous to the known ability of ClBcat to cleave C–O bonds in ethers.⁵⁵

As the mechanism depends on there being an excess of **1** with respect to PR₃, we presumed that the reaction of all of the

phosphines with an excess of **1** would cause the redistribution to take place. In order to investigate this, each of the phosphines was reacted with a five-fold excess of **1**. The reactions were monitored by *in situ* $^{11}\text{B}\{^1\text{H}\}$ NMR spectroscopy and all showed peaks due to **1** and **4**, and doublets due to **5a–g**. Additionally, 1 h after treatment of ClBcat with PMe_3 and PEt_3 , doublets were observed at δ 4.0 ($J_{\text{B-P}} = 183$ Hz) and δ 4.1 ($J_{\text{B-P}} = 175$ Hz) respectively. We believe that these additional low frequency resonances, which disappear after 24 h, may be due to the four-coordinate boron intermediates **6a** and **6b**, shown in Scheme 3. The resonance for the three-coordinate boron is likely to be superimposed on that for B_2cat_3 . The enhanced stability for such a species as an intermediate for PMe_3 and PEt_3 may be due to the smaller size of these phosphines.

Since the boron substituent redistribution yields B_2cat_3 , we postulated that the complicated $^{11}\text{B}\{^1\text{H}\}$ NMR spectrum obtained for the reaction of **1** with PCy_3 was the result of some interaction between PCy_3 and B_2cat_3 , **4**. Six reactions were conducted between B_2cat_3 and 0.1, 1, and 2 equivalents of either PEt_3 or PCy_3 . The *in situ* $^{11}\text{B}\{^1\text{H}\}$ NMR spectra of the reactions using PEt_3 showed a shift of approximately 2 ppm to lower frequency from the expected position of free **4**, indicating that some interaction between PEt_3 and **4** is taking place. This is confirmed by the $^{31}\text{P}\{^1\text{H}\}$ NMR spectra, which show broad singlets shifted by *ca.* 20 ppm to higher frequency from the position of free PEt_3 . The NMR spectra of the reactions with PCy_3 , however, clearly show that a reaction is taking place. The $^{11}\text{B}\{^1\text{H}\}$ NMR spectra show the formation of a sharp peak at δ 15.0, consistent with the $[\text{Bcat}_2]^-$ anion, a sharp peak at δ -14.8, and also other, as yet unassigned peaks, which are consistent with those observed for the reaction between PCy_3 and **4**. Removal of the solvent from the 2 : 1 PCy_3 : B_2cat_3 reaction followed by recrystallisation yielded single crystals, the X-ray diffraction analysis of which, though there was disorder, clearly showed the $[\text{Bcat}_2]^-$ anion and the $[\text{HPCy}_3]^+$ phosphonium cation.⁵⁶ No other products were isolated from any of the reactions with PCy_3 . The behaviour of PCy_3 is unique both in terms of reactivity and structure of the ClBcat adduct; the reasons for this are still elusive. However, it would appear that PCy_3 is sufficiently nucleophilic to displace $[\text{Bcat}_2]^-$ from B_2cat_3 .

To investigate the effect of nitrogen σ -donors, reactions of **1** with triethylamine, pyridine, 2-picoline and 4-picoline were carried out. The *in situ* $^{11}\text{B}\{^1\text{H}\}$ NMR spectra all showed broad peaks, shifted to lower frequency from the position of free **1**. The reactions all proceed cleanly, and no evidence of any decomposition was observed. Isolation of the pyridine and picoline adducts as solids proved difficult, as they tend to form oils, but removal of the solvent from the reaction with triethylamine and recrystallisation yielded single crystals of $\text{Et}_3\text{N}\cdot\text{ClBcat}$ **3h** suitable for X-ray structural analysis.

The molecular structure of **3h** (Fig. 10) shows a B–Cl bond length of 1.876(1) Å which is shorter than the B–Cl bond lengths in any of the phosphine adducts, the shortest of which is 1.911(2) Å in **3a**. This is most probably due to a combination of the smaller size of nitrogen vs. phosphorus, reducing steric interactions, and the larger electronegativity of nitrogen. The B–N bond of 1.643(1) Å is considerably shorter than the B–P bond lengths in any of the adducts, as expected, again due to the smaller size of nitrogen.

In the case of **3h**, NMR analysis of the adduct kept both in solution and in the solid state showed no redistribution to $\text{Et}_3\text{N}\cdot\text{BCl}_3$ and **4**, so this adduct appears to be thermally stable.

Conclusion

Phosphine adducts of ClBcat can be isolated only if the phosphine is of sufficient basicity, the less basic phosphines used causing the rapid redistribution of ClBcat to B_2cat_3 and the $\text{R}_3\text{P}\cdot\text{BCl}_3$ adduct. The redistribution depends on there being

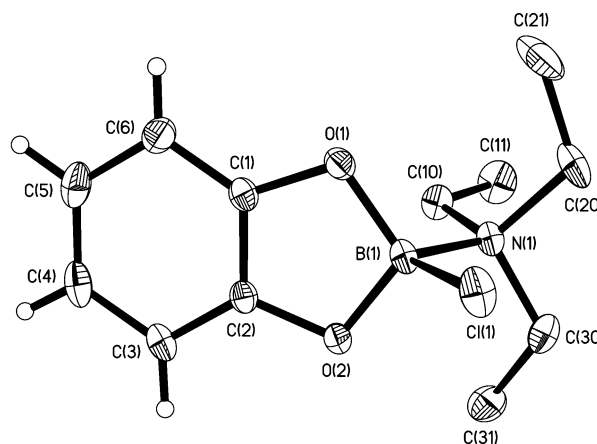


Fig. 10 Structure of $\text{Et}_3\text{N}\cdot\text{ClBcat}$ **3h**. Hydrogens on the Et groups omitted for clarity.

free **1** in solution. The less associated adducts derived from the less basic phosphines provide a larger concentration of **1** through dissociation leading to more rapid redistribution. Even those phosphine adducts that were observed or isolated were only kinetically stable, as redistribution took place slowly even in the solid state at -30 °C. In the case of PCy_3 , the phosphine reacts with the B_2cat_3 formed by the redistribution reaction. The presence of an excess of ClBcat relative to any of the phosphines causes the rapid boron substituent redistribution.

The nitrogen σ -donors formed stable adducts with ClBcat with no redistribution observed, either in the solid state or in solution, over an extended period of time.

Oxidative addition of ClBcat to low-valent, late transition metal phosphine complexes is known.⁴⁶ However, if labile phosphine ligands are employed in a catalytic process, reaction according to Scheme 3 is to be expected. This may, in fact, be valuable, in so far as it would inhibit re-coordination of the phosphine to the metal centre, with BCl_3 serving as an *in situ* phosphine sponge. It will be important to show that B_2cat_3 and $\text{R}_3\text{P}\cdot\text{BCl}_3$ will not otherwise interfere with any catalytic process.

Strong binding of amine bases to ClBcat may serve to inhibit phosphine-promoted redistribution reactions. Examination of the oxidative addition of the B–Cl bond in amine adducts such as **3h** to low-valent late transition metals will be the basis for subsequent reports.

Experimental

Air-sensitive compounds were manipulated in a nitrogen atmosphere using Schlenk techniques or in Innovative Technology, Inc. System 1 glove boxes. NMR spectra (at room temperature except where stated) were recorded on Bruker AC 200 (^{13}C), Varian Mercury 200 (^1H , ^{31}P), Varian Unity 300 (^1H , ^{11}B) and Varian Unity Inova 500 (^{11}B and VT ^{11}B) instruments. Variable temperature ^{31}P NMR experiments were conducted on a Varian VXR-400 instrument. Proton and ^{13}C NMR spectra were referenced to external SiMe_4 via residual protons in the deuterated solvents or solvent resonances respectively; ^{11}B and ^{31}P shifts were referenced to external $\text{BF}_3\cdot\text{OEt}_2$ and 85% H_3PO_4 , respectively. Elemental analyses were conducted in the Department of Chemistry at the University of Durham using an Exeter Analytical Inc. CE-440 Elemental Analyzer. Toluene was dried and deoxygenated by passage through columns of activated alumina and BASF-R311 catalyst under argon pressure using a modified version of the Innovative Technology Inc. SPS-400 solvent purification system.⁵⁷ Chloroform and CDCl_3 were dried over calcium hydride, C_6D_6 was dried over potassium metal, and all were distilled under nitrogen. The B-chlorocatechol borane (Aldrich) was sublimed under vacuum before use. Phosphines were purchased from Aldrich or Strem Chemicals Inc. and were checked for purity by ^1H and $^{31}\text{P}\{^1\text{H}\}$

NMR spectroscopy before use. Triethylamine, pyridine and 2- and 4-picoline were purchased from Lancaster and were distilled from calcium hydride.

Preparation of Me₃P·ClBcat 3a

A solution of PMe₃ (0.030 g, 0.389 mmol) in toluene (1 cm³) was added to a solution of ClBcat (0.061 g, 0.389 mmol) in toluene (1 cm³) and the mixture was stirred for 1 h. The solvent was removed *in vacuo* to yield 0.081 g of a white powder. The product was recrystallised from a minimum amount of toluene to yield 0.078 g (87%) of a white, crystalline solid. ¹H NMR (CDCl₃): δ 6.79 (m, 4H, 1,2-O₂C₆H₄), 1.51 (d, 9H, P(CH₃)₃, J_{H-P} = 11 Hz); ¹¹B{¹H} NMR (PhMe-10% C₆D₆): δ 11.1 (s); (at -40 °C): δ 11.0 (d, J_{B-P} = 178 Hz); ³¹P{¹H} NMR (PhMe-10% C₆D₆): δ -27.9 (s); (at -40 °C): δ -24.9 (q, J_{P-B} = 175 Hz); ¹³C{¹H} NMR (CDCl₃): δ 150.5 (s, 1,2-O₂C₆H₄), 119.9 (s, 1,2-O₂C₆H₄), 110.3 (s, 1,2-O₂C₆H₄), 9.4 (s, br, P(CH₃)₃) (Found: C, 46.89; H, 5.78. C₉H₁₃O₂ClBP requires C, 46.91; H, 5.69%).

Preparation of Et₃P·ClBcat 3b

As for 3a using PEt₃ (0.038 g, 0.324 mmol) and ClBcat (0.050 g, 0.324 mmol). Yield 0.068 g (78%). ¹H NMR (CDCl₃): δ 6.78 (m, 4H, 1,2-O₂C₆H₄), 1.89 (dq, 6H, P(CH₂CH₃)₃, J_{H-P} = 11 Hz, J_{H-H} = 8 Hz), 1.22 (dt, 9H, P(CH₂CH₃)₃, J_{H-P} = 16 Hz, J_{H-H} = 8 Hz); ¹¹B{¹H} NMR (PhMe-10% C₆D₆): δ 11.4 (s); (at -40 °C): δ 11.3 (d, J_{B-P} = 167 Hz); ³¹P{¹H} NMR (PhMe-10% C₆D₆): δ 1.4 (s); (at -40 °C) δ 6.8 (q, J_{P-B} = 169 Hz); ¹³C{¹H} NMR (CDCl₃): δ 150.2 (s, 1,2-O₂C₆H₄), 119.8 (s, 1,2-C₆H₄), 110.3 (s, 1,2-O₂C₆H₄), 10.5 (d, P(CH₂CH₃)₃, J_{C-P} = 34 Hz), 6.4 (d, P(CH₂CH₃)₃, J_{C-P} = 5 Hz) (Found: C, 52.60; H, 7.09. C₁₂H₁₉O₂ClBP requires C, 52.89; H, 7.03%).

Preparation of Me₂PhP·ClBcat 3c

As for 3a using PMe₂Ph (0.045 g, 0.324 mmol) and ClBcat (0.050 g, 0.324 mmol). Yield 0.075 g (79%). ¹H NMR (CDCl₃): δ 7.65 (m, 2H, PMe₂(C₆H₅)), 7.46 (m, 3H, PMe₂(C₆H₅)), 6.83 (m, 2H, 1,2-O₂C₆H₄), δ 6.74 (m, 2H, 1,2-O₂C₆H₄) δ 1.51 (d, 6H, P(CH₃)₂Ph, J_{P-H} = 9 Hz); ¹¹B{¹H} NMR (PhMe-10% C₆D₆): δ 11.8 (s); (at -40 °C): δ 11.6 (d, J_{B-P} = 166 Hz); ³¹P{¹H} NMR (PhMe-10% C₆D₆) δ -29.8 (s), (at -40 °C): δ -22.8 (q, J_{P-B} = 166 Hz); ¹³C NMR (CDCl₃): δ 150.5 (s, 1,2-O₂C₆H₄), 131.5 (s, P(CH₃)₂Ph), 131.1 (d, P(CH₃)₂(C₆H₅), J_{C-P} = 11 Hz), 129.1 (d, P(CH₃)₂(C₆H₅), J_{C-P} = 11 Hz), 120.0 (s, 1,2-O₂C₆H₄), 110.4 (s, 1,2-O₂C₆H₄), 7.9 (d, P(CH₃)₂Ph, J_{C-P} = 29 Hz), the resonances of the *ipso* carbon of P(CH₃)₂(C₆H₅) were not observed (Found: C, 57.27; H, 5.39. C₁₄H₁₅O₂ClBP requires C, 57.49; H, 5.17%).

Preparation of Bu^t₃P·ClBcat 3d

As for 3a using PBu^t₃ (0.066 g, 0.324 mmol) and ClBcat (0.050 g, 0.324 mmol). The product was recrystallised from toluene layered with hexane to yield 0.095 g (82%) of a crystalline white solid. ¹H NMR (C₆D₆): δ 6.87 (m, 4H, 1,2-O₂C₆H₄), 1.29 (d, 27H, P(C(CH₃)₃)₃, J_{H-P} = 11 Hz); (at -40 °C): δ 1.65 (d, J_{H-P} = 15 Hz); ¹¹B{¹H} NMR (PhMe-10% C₆D₆): δ 15.8 (s); (at -40 °C) δ 12.1 (d, J_{B-P} = 158 Hz); ³¹P{¹H} NMR (PhMe-10% C₆D₆): δ 25.5 (s); (at -40 °C) δ 15.3 (q, J_{P-B} = 160 Hz); ¹³C{¹H} NMR (CDCl₃): δ 120.3 (s, 1,2-O₂C₆H₄), 110.8 (s, 1,2-O₂C₆H₄), 36.9 (d, P(C(CH₃)₃)₃, J_{C-P} = 27 Hz), 30.1 (s, P(C(CH₃)₃)₃), the resonances of C1 and C2 of 1,2-O₂C₆H₄ were not observed) (Found: C, 60.34; H, 8.78. C₁₈H₃₁O₂ClBP requires C, 60.61; H, 8.76%).

Reaction of ClBcat with PCy₃

A solution of PCy₃ (0.091 g, 0.321 mmol) in toluene (1 cm³) was added to a solution of ClBcat (0.050 g, 0.321 mmol) in toluene (1 cm³) and the mixture was stirred for 1 h, by which time a white precipitate had formed. The precipitate was collected by

filtration and was recrystallised from toluene layered with hexane to yield a white solid (0.129 g). ¹¹B{¹H} NMR (PhMe-10% C₆D₆): δ 23.4 (B₂cat₃), 21.4, 12.1 (Cy₃P·ClBcat), 11.1, 3.7 (d, J_{B-P} = 147 Hz, Cy₃P·BCl₃); ³¹P{¹H} NMR (PhMe-10% C₆D₆): δ -3.3 (Cy₃P·ClBcat).

Synthesis of Cy₃P·ClBcat 3e

A 2 mol% excess of PCy₃ (0.093 g, 0.330 mmol) in toluene (1 cm³) was added to a solution of ClBcat (0.050 g, 0.324 mmol) in toluene (1 cm³), giving a white precipitate which was collected by filtration and recrystallised from toluene layered with hexane, yielding white crystals (0.038 g) from which the single crystal for X-ray analysis was obtained. ¹¹B{¹H} NMR (PhMe-10% C₆D₆): δ 22.2, 12.2 (Cy₃P·ClBcat); (at -40 °C): δ 11.8 (d, J_{B-P} = 160 Hz); ³¹P{¹H} NMR (PhMe-10% C₆D₆): δ -3.3 (Cy₃P·ClBcat); (at -40 °C): δ -6.6, (q, J_{P-B} = 159 Hz); ¹³C{¹H} NMR (C₆D₆): δ 149.8 (s, 1,2-O₂C₆H₄), 119.8 (s, 1,2-O₂C₆H₄), 110.4 (s, 1,2-O₂C₆H₄), 30.1 (d, P(C₆H₁₁)₃, J_{C-P} = 26 Hz), 28.0 (s, P(C₆H₁₁)₃), 27.2 (d, P(C₆H₁₁)₃, J_{C-P} = 11 Hz), 25.8 (s, P(C₆H₁₁)₃).

Reaction of ClBcat with PPh₂Me

A solution of ClBcat (0.050 g, 0.324 mmol) in toluene (1 cm³) was added to a solution of PPh₂Me (0.065 g, 0.324 mmol) in toluene (1 cm³) which was then stirred for 1 h. Removal of solvent yielded a white precipitate (0.094 g). ¹¹B{¹H} NMR (PhMe-10% C₆D₆): δ 27.9 (Ph₂MeP·ClBcat), 23.2 (B₂cat₃), 4.3 (d, J_{B-P} = 153 Hz, Ph₂MeP·BCl₃); ³¹P{¹H} NMR (PhMe-10% C₆D₆): δ -7.3 (q, J_{P-B} = 155 Hz, Ph₂MeP·BCl₃).

Reaction of ClBcat with PPh₃

A solution of ClBcat (0.050 g, 0.324 mmol) in toluene (1 cm³) was added to a solution of PPh₃ (0.084 g, 0.324 mmol) in toluene (1 cm³) which was then stirred for 1 h. Removal of solvent yielded a white precipitate (0.118 g). ¹¹B{¹H} NMR (PhMe-10% C₆D₆): δ 27.9 (s, Ph₃P·ClBcat), 23.1 (br s, B₂cat₃), 4.4 (d, J_{B-P} = 152 Hz, Ph₃P·BCl₃); ³¹P{¹H} NMR (PhMe-10% C₆D₆): δ 2.0 (q, J_{P-B} = 152 Hz, Ph₃P·BCl₃).

Preparation of Et₃N·ClBcat 3h

A solution of NEt₃ (0.033 g, 0.324 mmol) in CHCl₃ (1 cm³) was reacted with ClBcat (0.050 g, 0.324 mmol) in CHCl₃ (1 cm³) and the mixture was stirred for 1 h. The solvent was removed *in vacuo* leaving a white powder which was recrystallised from a minimum amount of CHCl₃ to yield 0.072 g (87%) of a crystalline white solid. ¹H NMR (CDCl₃): δ 6.89 (m, 4H, 1,2-O₂C₆H₄), 2.56 (q, 6H, N(CH₂CH₃)₃, J_{H-H} = 8 Hz), 0.71 (t, 9H, N(CH₂CH₃)₃, J_{H-H} = 8 Hz); ¹¹B{¹H} NMR (CDCl₃): δ 13.3 (s) (Found: C, 56.69; H, 7.59; N, 5.56. C₁₂H₁₉BCINO₂ requires C, 56.40; H, 7.49, N, 5.48%).

Preparation of C₅H₅N·ClBcat

A solution of C₅H₅N (0.025 g, 0.324 mmol) in CHCl₃ (1 cm³) was reacted with ClBcat (0.050 g, 0.324 mmol) in CHCl₃ (1 cm³) and the mixture was stirred for 1 h. ¹¹B{¹H} NMR (*in situ* CHCl₃-CDCl₃): δ 11.8 (C₅H₅N·ClBcat).

Preparation of 2-MeC₅H₄N·ClBcat

As for C₅H₅N·ClBcat using 2-MeC₅H₄N (0.030 g, 0.324 mmol) in CHCl₃ (1 cm³). ¹¹B{¹H} NMR (*in situ* CHCl₃-CDCl₃): δ 11.7 (2-CH₃C₅H₄N·ClBcat).

Preparation of 4-MeC₅H₄N·ClBcat

As for C₅H₅N·ClBcat using 4-MeC₅H₄N (0.030 g, 0.324 mmol) in CHCl₃ (1 cm³). ¹¹B{¹H} NMR (*in situ* CHCl₃-CDCl₃): δ 11.7 (4-MeC₅H₄N·ClBcat).

Table 4 Crystal data and structure refinement for ClBCat, BrBCat and the R₃P and Et₃N adducts of ClBCat

	ClBCat 1	BrBCat 2	Me ₃ P·ClBCat 3a	Et ₃ P·ClBCat 3b	Bu ^t ₃ P·ClBCat 3d	Cy ₃ P·ClBCat 3e	Et ₃ N·ClBCat 3h
Formula	C ₆ H ₄ BClO ₂	C ₆ H ₄ BBrO ₂	C ₉ H ₁₃ BClO ₂ P	C ₁₂ H ₁₉ BClO ₂ P	C ₁₈ H ₃₁ BClO ₂ P	C ₂₄ H ₃₇ BClO ₂ P	C ₁₂ H ₁₉ BClO ₂ N
<i>M</i>	154.35	198.81	230.42	272.50	356.66	434.77	255.54
<i>T</i> /K	120(2)	120(2)	160(2)	200(2)	120(2)	150(2)	100(2)
Crystal system	Monoclinic	Monoclinic	Monoclinic	Orthorhombic	Orthorhombic	Monoclinic	Orthorhombic
Space group	<i>C2/c</i>	<i>C2/c</i>	<i>P2₁/c</i>	<i>Pbca</i>	<i>Pna2₁</i>	<i>P2₁/n</i>	<i>P2₁2₁2₁</i>
<i>a</i> /Å	10.5584(8)	10.7250(4)	12.2244(10)	13.4416(12)	16.664(1)	11.541(2)	6.6037(3)
<i>b</i> /Å	9.8180(8)	10.0682(4)	16.3667(14)	14.0419(12)	13.455(5)	13.426(3)	13.3458(7)
<i>c</i> /Å	7.1370(5)	7.2078(3)	12.7944(11)	14.6040(12)	8.546(1)	15.070(3)	15.0557(7)
β /°	118.75(1)	119.53(1)	117.195(2)	90	90	92.226(3)	90
<i>U</i> /Å ³	648.62(9)	677.2(2)	2276.8(3)	2756.4(4)	1916.1(8)	2333.3(8)	1326.88(11)
<i>Z</i>	4	4	8	8	4	4	4
μ /mm ⁻¹	0.506	5.992	0.447	0.380	0.289	0.250	0.277
Reflections measured	2888	3032	14114	27702	14595	28034	15865
Unique reflections	753	914	5258	3169	4570	6574	3762
<i>R</i> _{int}	0.0319	0.0250	0.0349	0.1318	0.0242	0.0403	0.0152
<i>wR</i> ₂ (all data, on <i>F</i> ²)	0.0950	0.0637	0.0842	0.1059	0.0598	0.1055	0.0640
<i>R</i> [data with <i>F</i> ² > 2σ(<i>F</i> ²)]	0.0345	0.0243	0.0317	0.0393	0.0257	0.0395	0.0234

Computational study

Ab initio computations on R₃P·ClBCat adducts were carried out with the Gaussian 94 package.⁵³ The experimental geometries were fully optimised initially at the HF/3-21G level and then at the HF/6-31G* level with no symmetry constraints. Frequency calculations were computed on these optimised geometries at the HF/6-31G* level and no imaginary frequencies were found. For single point energies of the experimental geometries in Table 3, the hydrogens were first optimised at the HF/6-31G* level.

Crystallography

X-Ray diffraction experiments were carried out on a Bruker SMART three-circle diffractometer with a 1K CCD area detector, using graphite-monochromated Mo-Kα radiation ($\lambda = 0.71073$ Å) and a Cryostream (Oxford Cryosystems) open-flow N₂ gas cryostat. At least a hemisphere of data was collected in each case. Semi-empirical absorption corrections, by comparison of Laue equivalents, were applied (except for **3b**) using SADABS or XPREP programs.^{58,59} The structures were solved by direct methods and refined by full-matrix least squares against *F*² of all data, using SHELXTL software.⁵⁹ All non-H atoms were refined in anisotropic, H atoms in isotropic approximation. Compound **3a** crystallised with two independent molecules in the asymmetric unit which differ little in their geometries. Crystal data and experimental details are summarised in Table 4.

CCDC reference numbers 154920–154926.

See <http://www.rsc.org/suppdata/dt/b0/b010025k/> for crystallographic data in CIF or other electronic format.

Acknowledgements

We acknowledge EPSRC for research support (T. B. M. and J. A. K. H.), a Senior Research Fellowship (J. A. K. H.), an Advanced Research Fellowship (M. A. F.), an equipment grant (W. C.), and postgraduate studentships (R. B. C. and A. J. S.). We also acknowledge NSERC (Canada) for research support (T. B. M.) and a Postgraduate Fellowship (F. E. S. S.). We thank Prof. R. K. Harris and Dr A. M. Kenwright for helpful discussions on interpretation of some of the NMR spectra, Mr I. H. McKeag and Mrs C. F. Heffernan for assistance with the acquisition of low temperature NMR spectra, and Mrs J. Dostal for the elemental analyses.

References

- 1 K. Burgess and M. J. Ohlmeyer, *Chem. Rev.*, 1991, **91**, 1179.

- 2 A. H. Hoveyda, D. A. Evans and G. C. Fu, *Chem. Rev.*, 1993, **93**, 1307.
- 3 I. Beletskaya and A. Pelter, *Tetrahedron*, 1997, **53**, 4957.
- 4 T. B. Marder and N. C. Norman, *Top. Catal.*, 1998, **5**, 63.
- 5 T. Ishiyama and N. Miayaura, *J. Organomet. Chem.*, 2000, **611**, 392.
- 6 J. M. Brown and G. C. Lloyd-Jones, *J. Chem. Soc., Chem. Commun.*, 1992, 710.
- 7 K. Burgess, W. A. van der Donk, S. A. Westcott, T. B. Marder, R. T. Baker and J. C. Calabrese, *J. Am. Chem. Soc.*, 1992, **114**, 9350.
- 8 S. A. Westcott, T. B. Marder and R. T. Baker, *Organometallics*, 1993, **12**, 975.
- 9 J. M. Brown and G. C. Lloyd-Jones, *J. Am. Chem. Soc.*, 1994, **116**, 866.
- 10 R. T. Baker, J. C. Calabrese, S. A. Westcott and T. B. Marder, *J. Am. Chem. Soc.*, 1995, **117**, 8777.
- 11 D. H. Motry and M. R. Smith, III, *J. Am. Chem. Soc.*, 1995, **117**, 6615.
- 12 D. R. Lantero, D. L. Ward and M. R. Smith, III, *J. Am. Chem. Soc.*, 1997, **119**, 9699.
- 13 D. H. Motry, A. G. Brazil and M. R. Smith, III, *J. Am. Chem. Soc.*, 1997, **119**, 2743.
- 14 T. M. Cameron, R. T. Baker and S. A. Westcott, *Chem. Commun.*, 1998, 2395.
- 15 M. Murata, S. Watanabe and Y. Masuda, *Tetrahedron Lett.*, 1999, **40**, 2585.
- 16 C. M. Vogels, P. G. Hayes, M. P. Shaver and S. A. Westcott, *Chem. Commun.*, 2000, 51.
- 17 M. Suiginome, H. Nakamura and Y. Ito, *Chem. Commun.*, 1996, 2777.
- 18 S.-Y. Onozawa, Y. Hatanaka and M. Tanaka, *Chem. Commun.*, 1997, 1229.
- 19 T. Ishiyama, K. Nishijima, N. Miayaura and A. Suzuki, *J. Am. Chem. Soc.*, 1993, **115**, 7219.
- 20 Q. Cui, D. G. Musaev and K. Morokuma, *Organometallics*, 1998, **17**, 1383.
- 21 I. Beletskaya and C. Moberg, *Chem. Rev.*, 1999, **99**, 3435.
- 22 S.-Y. Onozawa, Y. Hatanaka, T. Sakakura, S. Shimada and M. Tanaka, *Organometallics*, 1996, **15**, 5450.
- 23 S.-Y. Onozawa, Y. Hatanaka, N. Choi and M. Tanaka, *Organometallics*, 1997, **16**, 5389.
- 24 N. Miayaura and A. Suzuki, *Chem. Rev.*, 1995, **95**, 2457.
- 25 T. Ishiyama, M. Murata and N. Miayaura, *J. Org. Chem.*, 1995, **60**, 7508.
- 26 M. Murata, S. Watanabe and Y. Masuda, *J. Org. Chem.*, 1997, **62**, 6458.
- 27 S. R. Piettre and S. Baltzer, *Tetrahedron Lett.*, 1997, **38**, 1197.
- 28 T. Ishiyama, Y. Itoh, T. Kitamo and N. Miayaura, *Tetrahedron Lett.*, 1997, **38**, 3447.
- 29 A. Suzuki, *J. Organomet. Chem.*, 1999, **576**, 147.
- 30 T. Ishiyama and N. Miayaura, *J. Synth. Org. Chem., Jpn.*, 1999, **57**, 395.
- 31 T. Ishiyama and N. Miayaura, *Chem. Lett.*, 2000, 126.
- 32 M. Murata, S. Watanabe and Y. Masuda, *Tetrahedron Lett.*, 2000, **41**, 5877.
- 33 M. Murata, T. Oyama, S. Watanabe and Y. Masuda, *J. Org. Chem.*, 2000, **65**, 164.

- 34 H. Nakamura, M. Fujiwara and Y. Yamamoto, *Bull. Chem. Soc. Jpn.*, 2000, **73**, 231.
- 35 K. M. Waltz, X. He, C. Muhoro and J. F. Hartwig, *J. Am. Chem. Soc.*, 1995, **117**, 11357.
- 36 K. M. Waltz and J. F. Hartwig, *Science*, 1997, **277**, 211.
- 37 C. N. Iverson and M. R. Smith, III, *J. Am. Chem. Soc.*, 1999, **121**, 7696.
- 38 K. M. Waltz, C. N. Muhoro and J. F. Hartwig, *Organometallics*, 1999, **18**, 3383.
- 39 H. Chen and J. F. Hartwig, *Angew. Chem., Int. Ed. Engl.*, 1999, **38**, 3391.
- 40 H. Chen, S. Scheldt, T. C. Semple and J. F. Hartwig, *Science*, 2000, **287**, 1995.
- 41 S. Shimada, A. S. Batsanov, J. A. K. Howard and T. B. Marder, *Angew. Chem., Int. Ed.*, in the press.
- 42 H. Wadepohl, *Angew. Chem., Int. Ed. Engl.*, 1997, **36**, 2441.
- 43 H. Braunschweig, *Angew. Chem., Int. Ed.*, 1998, **37**, 1786.
- 44 G. J. Irvine, M. J. G. Lesley, T. B. Marder, N. C. Norman, C. R. Rice, E. G. Robins, W. R. Roper, G. R. Whittell and L. J. Wright, *Chem. Rev.*, 1998, **98**, 2685.
- 45 M. R. Smith, III, *Prog. Inorg. Chem.*, 1999, **48**, 505.
- 46 W. Clegg, F. J. Lawlor, G. Lesley, T. B. Marder, N. C. Norman, A. G. Orpen, M. J. Quayle, C. R. Rice, A. J. Scott and F. E. S. Souza, *J. Organomet. Chem.*, 1998, **550**, 183.
- 47 D. Männig and H. Nöth, *J. Chem. Soc., Dalton Trans.*, 1985, 1689.
- 48 C. Einertshofer, PhD Thesis, Ludwig-Maximilians Universität, Munich, 1992.
- 49 S. A. Westcott, H. P. Blom, T. B. Marder, R. T. Baker and J. C. Calabrese, *Inorg. Chem.*, 1993, **32**, 4367.
- 50 J. M. Burke, F. E. S. Souza, A. S. Batsanov, C. Wilson, D. S. Yufit, J. A. K. Howard, L. Horsburgh, W. Clegg and T. B. Marder, *J. Chem. Soc., Dalton Trans.*, in preparation.
- 51 M. M. Rahman, H.-Y. Liu, K. Eriks, A. Prock and W. P. Giering, *Organometallics*, 1989, **8**, 1.
- 52 C. A. Tolman, *Chem. Rev.*, 1977, **77**, 313.
- 53 Gaussian 94: M. J. Frisch, G. W. Trucks, H. B. Schlegel, P. M. W. Gill, B. G. Johnson, M. A. Robb, J. R. Cheeseman, T. Kieth, G. A. Petersson, J. A. Montgomery, K. Raghavachari, M. A. Al-Laham, V. G. Zakrzewski, J. V. Ortiz, J. B. Foresman, J. Cioslowski, B. B. Stefanov, A. Nanayakkara, M. Challacombe, C. Y. Peng, P. Y. Ayala, W. Chen, M. W. Wong, J. L. Andres, E. S. Replogle, R. Gomperts, R. L. Martin, D. J. Fox, J. S. Binkley, D. J. Defrees, J. Baker, J. P. Stewart, M. Head-Gordon, C. Gonzalez and J. A. Pople, Gaussian Inc., Pittsburgh, PA, 1995.
- 54 3D Search and Research Using the Cambridge Structural Database, F. H. Allen and O. Kennard, *Chem. Des. Automat. News*, 1993, **8**, 1; F. H. Allen and O. Kennard, *Chem. Des. Automat. News*, 1993, **8**, 31.
- 55 R. K. Boeckman and J. C. Potenza, *Tetrahedron Lett.*, 1985, **26**, 1411.
- 56 For related structures of $[\text{HPMe}_3]^+[\text{Bcat}_2]^-$ see: W. Clegg, A. J. Scott, F. J. Lawlor, N. C. Norman, T. B. Marder, C. Dai and P. Nguyen, *Acta Crystallogr., Sect. C*, 1998, **54**, 1875.
- 57 A. B. Pangborn, M. A. Giardello, R. H. Grubbs, R. K. Rosen and F. J. Timers, *Organometallics*, 1996, **15**, 1518.
- 58 G. M. Sheldrick, SADABS: Program for scaling and correction of area detector data, University of Göttingen, Germany, 1996.
- 59 SHELXTL, An integrated system for solving, refining, and displaying crystal structures from diffraction data, Ver. 5.10, Bruker Analytical X-ray Systems, Madison, WI, USA, 1997.